

Electrodeposition of Aluminum–Tungsten Alloy Films Using EMIC–AlCl₃–W₆Cl₁₂ Ionic Liquids of Different Compositions

Shota Higashino^{1,*1}, Masao Miyake^{1,*2}, Hisashi Fujii¹,
Ayumu Takahashi¹, Ryuta Kasada² and Tetsuji Hirato¹

¹Graduate School of Energy Science, Kyoto University, Kyoto 606-8501, Japan

²Institute for Materials Research, Tohoku University, Sendai 980-8577, Japan

Electrodeposition of Al–W alloy films with high W contents has been carried out using 1-ethyl-3-methylimidazolium chloride (EMIC)–aluminum chloride (AlCl₃) ionic liquids containing tungsten(II) chloride (W₆Cl₁₂). Although the corrosion resistance and hardness of the alloy films are expected to be improved with an increase in the W content, dense films with W contents higher than ~12 at% have not been obtained by electrodeposition to date. This study has demonstrated that electrodeposition using a EMIC–AlCl₃–W₆Cl₁₂ bath with a lower AlCl₃/EMIC molar ratio can yield Al–W alloys with higher W contents. The maximum W content of the alloys electrodeposited using the EMIC–1.5AlCl₃ bath reached 19.4 at%. The alloy films with up to ~18 at% W were dense and smooth, whereas those with >~18 at% W exhibited increased surface roughness. The hardness and Young's modulus of the dense and smooth 17.7 at% W film were determined by nano-indentation. The hardness of this film was confirmed to be higher than those of the Al–W alloy films previously obtained from the EMIC–2AlCl₃ baths.

[doi:10.2320/matertrans.M2018051]

(Received February 6, 2018; Accepted April 2, 2018; Published May 11, 2018)

Keywords: electroplating, aluminum alloy, tungsten, ionic liquid, nano-indentation

1. Introduction

Aluminum alloys have attracted significant research attention as corrosion-protective coatings for reactive metallic materials such as magnesium alloys.^{1,2)} In particular, aluminum–tungsten (Al–W) alloys are known to have the highest resistance to pitting corrosion among Al-based binary alloys.^{3,4)} Many researchers have studied the formation of Al–W alloy films by using sputtering,^{3–10)} electrodeposition,^{11–16)} ion implantation,¹⁷⁾ and laser alloying.¹⁸⁾ Among these methods, electrodeposition is advantageous in that a thick film can be rapidly formed on a large substrate with simple equipment. A number of studies on the electrodeposition of Al and Al alloys in molten salts,^{1,19,20)} ionic liquids,^{21–25)} and organic solvents^{26–35)} have been reported. Several review articles are available in literature.^{36–42)} Recently, electrodeposition using ionic liquids such as 1-ethyl-3-methylimidazolium chloride (EMIC)–aluminum chloride (AlCl₃) has become popular because of their low melting point and vapor pressure.⁴³⁾

Electrodeposition of Al–W alloy films with high W contents has been pursued using an EMIC–2AlCl₃ ionic liquid (AlCl₃/EMIC = 2 in molar ratio) containing a W precursor. EMIC–2AlCl₃ ionic liquids containing K₃W₂Cl₉ yielded Al–W alloys with >15 at% W.¹³⁾ However, the alloys from these baths had a powdery morphology when the W content exceeded 3 at%. In contrast, when the W precursor was replaced with tungsten(II) chloride, W₆Cl₁₂, dense Al–W alloy films with up to ~12 at% W were successfully electrodeposited.^{15,16)} The resultant dense films were confirmed to exhibit a good corrosion resistance.

In terms of practical application as corrosion-protective coatings, it is preferable that the coatings have not only a high corrosion resistance but also a high mechanical strength.

Wear resistance of a coating material can be predicted from its hardness and the ratio of hardness to Young's modulus.^{44,45)} We have previously examined Al–W alloy films with up to ~12 at% W for hardness and Young's modulus, and showed that these alloy films are harder and have a higher ratio of hardness to Young's modulus than Al metal.¹⁶⁾ This study suggested that Al–W alloy films with a higher W content could have an even higher mechanical strength.

However, Al–W alloy films with W contents higher than ~12 at% could not be electrodeposited using EMIC–2AlCl₃–W₆Cl₁₂ baths.¹⁶⁾ The W content of the alloy films electrodeposited at a constant current density increased linearly up to ~12 at% with increasing W₆Cl₁₂ concentration of the bath in a low W₆Cl₁₂ concentration range, but the W content of the films saturated at ~12 at% at a higher W₆Cl₁₂ concentration. Potentiostatic electrodeposition at various potentials in an EMIC–2AlCl₃ bath saturated with W₆Cl₁₂ also failed to yield alloy films with >~12 at% W.¹⁵⁾

One of the parameters that have not yet been explored in this system is the AlCl₃/EMIC molar ratio of the bath. A decrease in the AlCl₃/EMIC molar ratio below the previously tested value of 2 is expected to suppress the electrodeposition rate of Al, and therefore, increase the W content of the resulting films. In the present study, electrodeposition in EMIC–AlCl₃–W₆Cl₁₂ baths with an AlCl₃/EMIC molar ratio of 1.5 was carried out to obtain Al–W alloy films with a higher W content. The surface morphology, crystal structure, hardness, and Young's modulus of the electrodeposited films were investigated.

2. Experimental Procedure

Electrochemical experiments using EMIC–AlCl₃–W₆Cl₁₂ baths were carried out in an argon-filled glove box (SDB-1AO, MIWA MFG). The electrolytic bath was prepared by adding anhydrous aluminum chloride (AlCl₃, 99%, Fluka) to

*1Graduate Student, Kyoto University

*2Corresponding author, E-mail: miyake.masao.4e@kyoto-u.ac.jp

EMIC (97%, Tokyo Chemical Industry) in a molar ratio of AlCl₃:EMIC = 1.5:1. The EMIC was dried under vacuum at 120°C prior to use. The prepared EMIC–AlCl₃ melt was stored in a 25-mL glass vessel used as an electrolytic cell. W₆Cl₁₂ was synthesized by a method described in our previous report,^{15,16} and was added to the melt maintained at 80°C throughout the experiment. The bath temperature was controlled by a thermostat (TJA-550, AS ONE) connected to a rubber heater wound around the cell and a thermocouple immersed in the bath.

Electrodeposition was performed on a polished copper (Cu) plate. A section of the Cu plate was covered with polytetrafluoroethylene tape so that a defined area (5 mm × 5 mm) was exposed to the bath. An Al plate was used as the counter electrode. An Al wire immersed in an EMIC–2AlCl₃ ionic liquid separated from the bath with a glass frit was used as the reference electrode. The Cu and Al plates were placed vertically and parallel to each other. The distance between the Cu and Al plates was less than 10 mm. During the electrodeposition process, the bath was agitated at 150 rpm using a magnetic stirrer (PC-420D, CORNING) and a stirrer bar (15 mm × 5 mm). The electrochemical experiments were carried out using an electrochemical analyzer (ALS 660c).

A scanning electron microscope (SEM; JEOL, JSM-6510LV) equipped with energy dispersive X-ray spectroscopy (EDX; INCAx-act, Oxford Instruments) was used to observe the morphology and determine the elemental composition of the deposit. X-ray diffraction (XRD) patterns were obtained with an X-ray diffractometer (X'pertPRO-MPD, PANalytical) using Cu K α radiation (wave length of 0.15405 nm).

The hardness and Young's modulus of the Al–W alloy films were measured by nano-indentation tests using a nano-indenter (G200, Agilent Technologies) with a diamond Berkovich tip. As the nano-indentation test sample, a ~10 μ m-thick Al–W alloy film with a selected composition was electrodeposited on a Ni plate. The surface of the 10 μ m-thick alloy film was polished prior to the indentation tests to minimize the errors caused by surface roughness. Hardness and Young's modulus data were collected using the continuous stiffness measurement technique^{46,47} with a vibration frequency of 45 Hz. In each indentation, the hardness and Young's modulus values were obtained at a depth of 200 nm, where the deformation of the substrate was not influential. Each value reported for the hardness and Young's modulus is an average of the values taken at 12 indentation points separated from each other by more than 50 μ m. In the evaluation of Young's modulus, Poisson's ratio of the Al–W alloy films was assumed to be 0.3, which is a typical value for metallic materials.⁴⁸ The error in Young's modulus caused by varying Poisson's ratio between 0.2 and 0.4 remains within 8%.⁴⁹

3. Results and Discussions

3.1 Electrolytic bath composition

Previous studies have shown that a maximum W content of ~12 at% could be obtained in Al–W alloy films electrodeposited in EMIC–AlCl₃–W₆Cl₁₂ baths where the AlCl₃/EMIC molar ratio was 2. In the present study,

Table 1 Bath compositions employed in our previous (bath A) and present studies (baths B and C).

Bath	EMIC:AlCl ₃ :W ₆ Cl ₁₂	W ₆ Cl ₁₂ concentration
	(molar ratio)	(mM)
A	1:2:0.015	49
B	1:1.5:0.015	56
C	1:1.5:0.027	105

electrodeposition was carried out using ionic liquids with a lower AlCl₃/EMIC molar ratio (1.5), with the aim of obtaining alloy films with a higher W content. The compositions of the electrolytic baths employed are shown in Table 1. In the EMIC–2AlCl₃ bath, which had been employed in the previous studies, W₆Cl₁₂ concentration reached saturation at 49 mM. The composition of this bath (bath A) is expressed as EMIC–2AlCl₃–0.015W₆Cl₁₂ in molar ratio. Bath B (EMIC–1.5AlCl₃–0.015W₆Cl₁₂ in molar ratio) has the lower AlCl₃/EMIC ratio of 1.5, while the W₆Cl₁₂/EMIC ratio is fixed at 0.015, as in bath A. The volume molar concentration of W₆Cl₁₂ in bath B is 56 mM, which is a little higher than, but almost the same as, that in bath A. We found that W₆Cl₁₂ was more soluble in EMIC–1.5AlCl₃ than in EMIC–2AlCl₃, with a W₆Cl₁₂ saturation concentration in EMIC–1.5AlCl₃ of 105 mM. The composition of this W₆Cl₁₂-saturated bath (bath C) is expressed as EMIC–1.5AlCl₃–0.027W₆Cl₁₂.

3.2 Electrodeposition and characterization

Electrodeposition was carried out using bath B to examine the influence of the lower AlCl₃/EMIC ratio (1.5) on the W content of the resulting Al–W alloy films. The charge for each electrodeposition experiment was set at 8 C cm^{–2}, which is the charge required for the electrodeposition of a 2.8 μ m Al film or a 3.9 μ m thick W film.

Figure 1 compares the current density vs. electrolysis potential plots obtained during electrodeposition in baths A and B. An Al wire immersed in an EMIC–2AlCl₃ ionic liquid separated from the bath with a porous glass frit was used as the reference electrode. In bath A, the current density increased with the decrease in the potential from –0.1 V, which is close to the equilibrium potential of Al (0 V). In bath B, a similar trend was observed, except that the current density observed for bath B was almost half of that for bath A at each potential. Previously, Al–W alloy films with <~12 at% W were electrodeposited in bath A at potentials of <–0.1 V, where the current efficiency was ~90%.¹⁵ Accordingly, about 80% of the current density observed for bath A at <–0.1 V is attributed to the deposition of Al. Therefore, the lower current density observed for bath B in comparison to bath A reflects the lower deposition rate of Al in bath B. This is reasonable because of the lower AlCl₃ concentration of bath B.

Electrodeposition in bath B at potentials more negative than –0.1 V produced deposits on the substrate. However, the deposits obtained at >–0.2 V were fragile and easily exfoliated from the substrate during the washing process, making further analysis impossible. A typical EDX spectrum

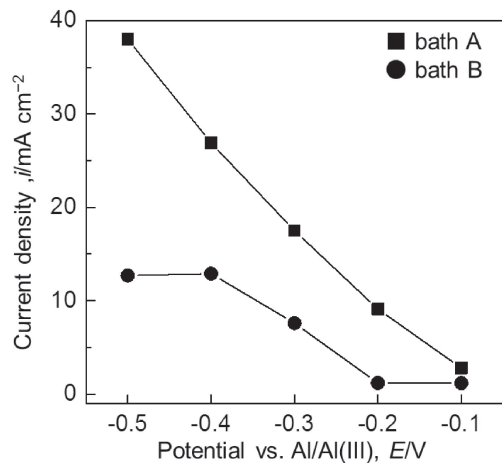


Fig. 1 Current density vs. electrolysis potential during electrodeposition in baths A and B.

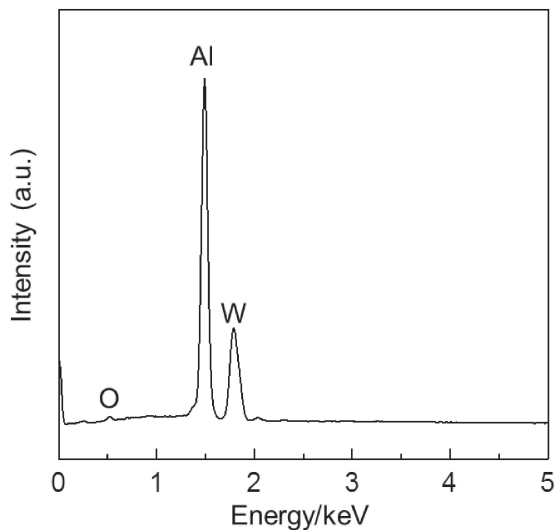


Fig. 2 EDX spectra of the electrodeposit in bath B at -0.2 V.

of the deposits obtained from bath B at < -0.2 V is shown in Fig. 2. The EDX spectrum indicates that the deposit is composed of Al and W, except for a small amount of O, which is derived from the surface oxidation layer, confirming that Al–W alloys can also be electrodeposited in bath B. The W content of the deposits determined by the EDX is shown in Fig. 3. The W content of the alloys obtained from bath B was higher than that from bath A at each potential. The maximum W content of the alloys obtained from bath B reached 15.7 at%, which was higher than that from bath A, ~ 12 at%.

With the aim of obtaining alloys with a further increase in W content, electrodeposition in an EMIC–1.5AlCl₃ bath saturated with W₆Cl₁₂ (bath C) was carried out. Deposits firmly adhering to the substrate could be obtained by electrodeposition at potentials < -0.2 V, as was the case in bath B; the deposits obtained at > -0.2 V were too fragile and easily washed away. The W contents of the alloys obtained at > -0.2 V are shown in Fig. 3. The W contents of the alloys obtained from bath C were higher than those of the alloys from bath B, and reached 19.4 at%, reflecting the higher W₆Cl₁₂ concentration in bath C in comparison to bath B.

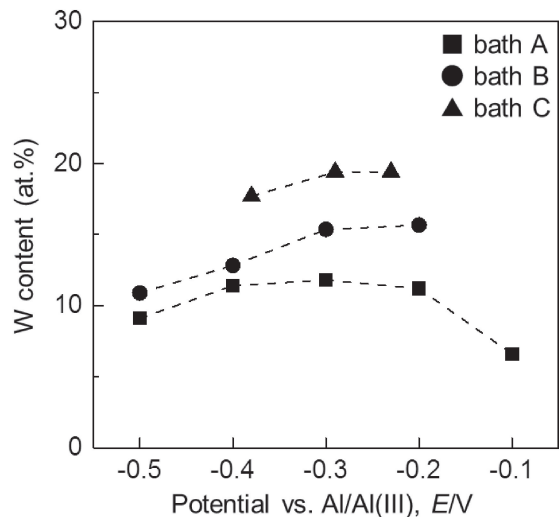


Fig. 3 W contents of electrodeposited Al–W alloy films vs. electrolysis potential during electrodeposition.

Figure 4 presents the typical surface SEM images of the alloys with > 15 at% W obtained from the EMIC–1.5AlCl₃ baths. These alloys are mainly composed of globular grains without defined facets. The alloys with W content up to ~ 18 at% exhibit a dense and relatively smooth morphology (Fig. 4(a)). However, the alloys with higher W contents, exceeding 18 at%, exhibit a rough surface with conical-shaped needle-like grains (Fig. 4(b)). Similar needle-like grains have also been observed in the electrodeposition of other Al-based alloys such as Al–Mo–Mn and Al–Mo–Ti.^{50,51} Although the detailed mechanism is not clear, the needle-like grains commonly tend to be formed when the electrodeposition is performed at a low overpotential (i.e., at a low deposition rate) in a bath with a high concentration of the ions of the alloy constituents. The formation of the needle-like grains may be attributed to the adsorption of the metal ions, which suppress the electrodeposition of Al onto the surface of the electrodeposit.

Figure 5 presents the typical XRD patterns of the alloy films with > 15 at% W obtained from the EMIC–1.5AlCl₃ baths. Apart from the diffraction peaks of the Cu substrate, the XRD patterns of these alloy films show only a halo at around $2\theta = 42^\circ$, indicating that these films are composed of an amorphous phase. Previous studies using EMIC–2AlCl₃ baths showed that the electrodeposited alloys with $< \sim 10$ at% W are composed of a single phase, a solid-solution of fcc Al containing W atoms; the alloys with $> \sim 10$ at% W comprise two phases, the fcc Al and an amorphous phase, with the proportion of the amorphous phase increasing with increasing W content; the alloys with ~ 12 at% W are composed of a single amorphous phase.¹⁶ The present results show that the single amorphous phase extends up to at least 19.4 at% W.

As described above, Al–W amorphous alloy films with high W contents exceeding ~ 12 at% were obtained by using baths with the low AlCl₃/EMIC molar ratio of 1.5. We also examined baths with an even lower AlCl₃/EMIC molar ratio of 1.2. However, alloys with a high W content could not be obtained because only a small amount of W₆Cl₁₂ dissolved in such baths.

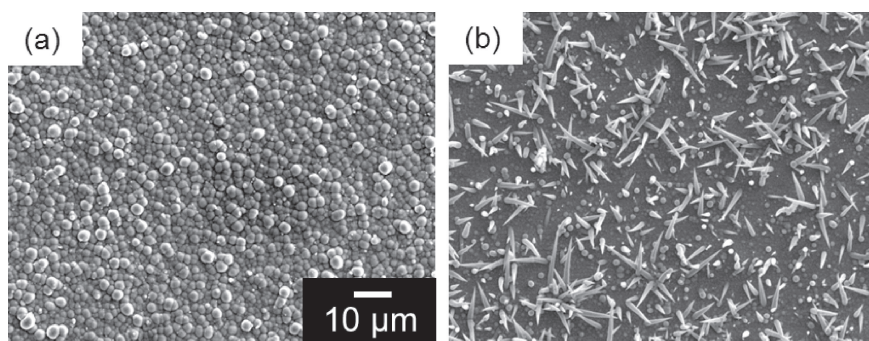


Fig. 4 Surface SEM images of Al–W alloy films with (a) 17.7 and (b) 19.4 at% W. These films were electrodeposited from bath C at potentials of -0.23 V and -0.38 V, respectively.

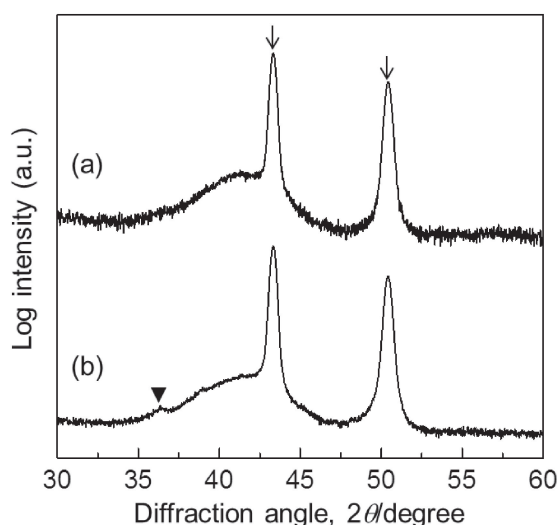


Fig. 5 Typical XRD patterns of Al–W alloy films with >15 at% W. The W contents are (a) 19.4 and (b) 17.7 at%. The arrows indicate the diffraction peaks from the Cu substrate. The solid triangle (▼) indicates the diffraction peak from Cu₂O, which is obtained from the oxidation of the Cu substrate.

3.3 Nano-indentation test

The hardness (H) and Young's modulus (E) values of a high W content film (17.7 at% W) were evaluated using nano-indentation. Although a higher W content alloy (19.4 at% W) was obtained, reliable data for this alloy could not be obtained from the nano-indentation test because of the increased surface roughness visible in Fig. 4(b).

The H and E values of the 17.7 at% W film are shown in Figs. 6(a) and (b). The figures also show the H and E values of the 0–12 at% W films reported previously.¹⁶⁾ The trend in the variation of the H and E values is explained by the W content and phase of the films. The H value of the <10 at% W films, which are single-phase fcc Al solid solutions, increases with increasing W content. The H value of the ~ 10 at% W film, where the fcc Al phase coexists with an amorphous phase, shows a local maximum. With a further increase in W content to ~ 12 at%, the presence of the amorphous phase increases and the H value slightly decreases. The variation in E is similar to that for the H values.

The 17.7 at% W film obtained in the present study is composed of a single amorphous phase, and its W content is higher than that of the single amorphous W film obtained previously (12 at%). The H and E values for the 17.7 at% W

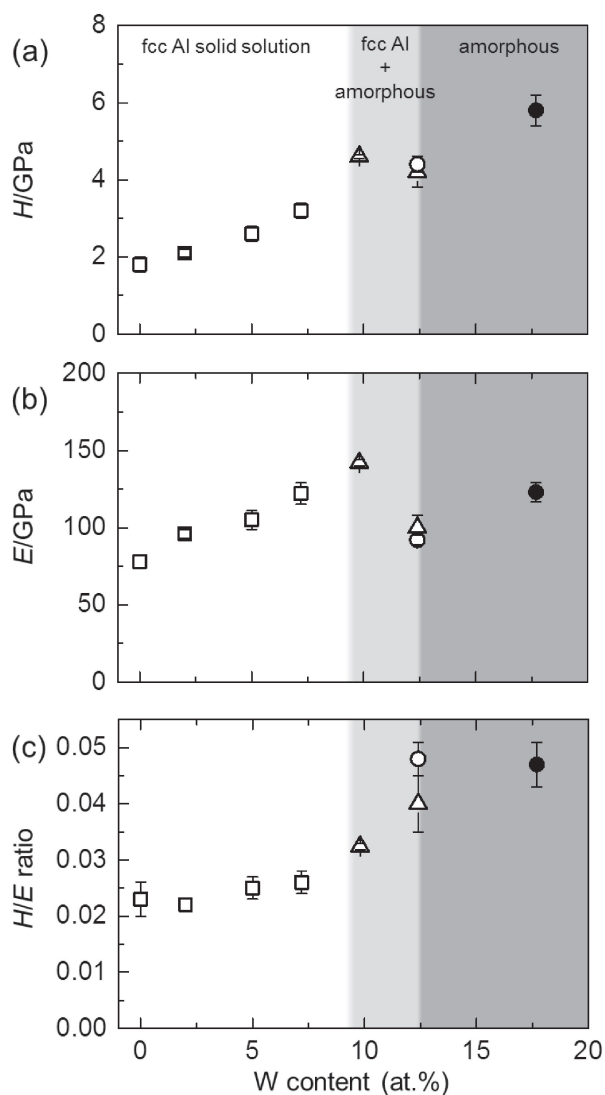


Fig. 6 (a) Hardness (H), (b) Young's modulus (E), and (c) H/E ratio of Al–W alloy films. Solid symbols indicate the data for the 17.7 at% W film, which was newly obtained in this study. The 17.7 at% W film was electrodeposited from bath C at potentials of -0.38 V. Square, triangle, and circle symbols represent the fcc Al solid solution phase, fcc Al + amorphous coexisting phase, and single amorphous phase, respectively.

films are higher than those for the ~ 12 at% W films. The increases in H and E values for the single amorphous films with increasing W content can be understood in terms of the average interatomic distance. As is the case with crystalline alloys, the elastic behavior of amorphous alloys depends on

the interatomic distance.^{48,52,53} A decrease in interatomic distance leads to stiffer interatomic bonding, resulting in a higher E value. In addition, the plastic deformation, which is related to H , of an amorphous alloy is considered to proceed by the propagation of shear displacement in a group of atoms wherein the interatomic distance is relatively large.^{54,55} Therefore, the decrease in the average interatomic distance increases the resistance to shear displacement, resulting in a higher H value.⁵⁶ Because W has a smaller atomic radius than Al, the average interatomic distance in Al–W alloy films should decrease with increasing content of W atoms.^{13,15,16} Therefore, the higher H and E values of the 17.7 at% W film in comparison to those of the ~12 at% W amorphous films are reasonable.

Coating materials with a high hardness (H) value and a high ratio of hardness to Young's modulus (H/E) are believed to have a high wear resistance. As shown in Figs. 6(a) and (c), the H value and H/E ratio of the 17.7 at% W film are higher than those of the <~12 at% W film containing the fcc Al phase. A comparison between the values of the single-phase amorphous films with ~12 at% W and 17.7 at% W proves that the H/E ratio is almost the same for these two films, but H value is higher for the 17.7 at% W film. Therefore, the 17.7 at% W film obtained in the present study is expected to have a higher resistance to mechanical damages than the films obtained previously.

4. Conclusion

Electrodeposition of Al–W alloys in EMIC–AlCl₃–W₆Cl₁₂ baths with AlCl₃/EMIC molar ratios lower than 2 was examined. W₆Cl₁₂ was more soluble in EMIC–1.5AlCl₃ than in EMIC–2AlCl₃, but was much less soluble in EMIC–1.2AlCl₃ bath. Electrodeposition in the EMIC–1.5AlCl₃ baths generated alloy films with up to 19.4 at% W, which was higher than those previously obtained from EMIC–2AlCl₃ baths (~12 at% W). The increase in W content for the EMIC–1.5AlCl₃ baths can be explained by the lower deposition ratio of Al and higher W₆Cl₁₂ concentration. Alloy films with up to ~18 at% W were dense and smooth, whereas those with >~18 at% W exhibited a rough surface. The hardness of the 17.7 at% W film was higher than those of the Al–W alloy films previously obtained from EMIC–2AlCl₃ baths, owing to the higher W content of the film. Young's modulus also increased with the increase in W content from 12 to 17.7 at%, while the ratio of hardness to Young's modulus remained almost constant.

Acknowledgments

This work was supported by JSPS KAKENHI [grant number 17H03429], and the “Joint Usage/Research Program on Zero-Emission Energy Research, Institute of Advanced Energy, Kyoto University (ZE28-C-7)”.

REFERENCES

- 1) J. Zhang, C. Yan and F. Wang: *Appl. Surf. Sci.* **255** (2009) 4926–4932.
- 2) T. Tokunaga, K. Sotomoto, M. Ohno and K. Matsuura: *Mater. Trans.* **59**

- (2018) 432–436.
- 3) B.A. Shaw, T.L. Fritz, G.D. Davis and W.C. Moshier: *J. Electrochem. Soc.* **137** (1990) 1317–1318.
- 4) B.A. Shaw, G.D. Davis, T.L. Fritz, B.J. Rees and W.C. Moshier: *J. Electrochem. Soc.* **138** (1991) 3288–3295.
- 5) G.D. Davis, B.A. Shaw, B.J. Rees and M. Ferry: *J. Electrochem. Soc.* **140** (1993) 951–959.
- 6) A. Wolowik, M. Janik-Czachor and Z. Werner: *Mater. Chem. Phys.* **49** (1997) 164–168.
- 7) A. Wolowik and M. Janik-Czachor: *Mater. Sci. Eng. A* **267** (1999) 301–306.
- 8) M. Stubičar, A. Tonejc and N. Radic: *Vacuum* **61** (2001) 309–316.
- 9) D. Kek Merl, P. Panjan and I. Milošev: *Surf. Eng.* **29** (2013) 281–286.
- 10) D. Kek Merl, P. Panjan and J. Kovač: *Corros. Sci.* **69** (2013) 359–368.
- 11) T. Tsuda, C.L. Hussey and G.R. Stafford: *ECS Trans.* **3** (2007) 217–231.
- 12) T. Tsuda, Y. Ikeda, T. Arimura, A. Imanishi, S. Kuwabata, C.L. Hussey and G.R. Stafford: *ECS Trans.* **50** (2013) 239–250.
- 13) T. Tsuda, Y. Ikeda, T. Arimura, M. Hirogaki, A. Imanishi, S. Kuwabata, G.R. Stafford and C.L. Hussey: *J. Electrochem. Soc.* **161** (2014) D405–D412.
- 14) K. Sato, H. Matsushima and M. Ueda: *ECS Trans.* **75** (2016) 305–312.
- 15) S. Higashino, M. Miyake, H. Fujii, A. Takahashi and T. Hirato: *J. Electrochem. Soc.* **164** (2017) D120–D125.
- 16) S. Higashino, M. Miyake, A. Takahashi, Y. Matamura, H. Fujii, R. Kasada and T. Hirato: *Surf. Coat. Tech.* **325** (2017) 346–351.
- 17) C.M. Rangel, M.A. Travassos and J. Chevallier: *Surf. Coat. Tech.* **89** (1997) 101–107.
- 18) R.S. Rajamure, H.D. Vora, S.G. Srinivasan and N.B. Dahotre: *Appl. Surf. Sci.* **328** (2015) 205–214.
- 19) M. Ueda, H. Kigawa and T. Ohtsuka: *Electrochim. Acta* **52** (2007) 2515–2519.
- 20) G.R. Stafford: *J. Electrochem. Soc.* **136** (1989) 635–639.
- 21) T. Tsuda, C.L. Hussey, G.R. Stafford and J.E. Bonevich: *J. Electrochem. Soc.* **150** (2003) C234–C243.
- 22) S. Ruan and C.A. Schuh: *Acta Mater.* **57** (2009) 3810–3822.
- 23) S.R. Cross and C.A. Schuh: *Electrochim. Acta* **211** (2016) 860–870.
- 24) S.J. Pan, W.T. Tsai, J.K. Chang and I.W. Sun: *Electrochim. Acta* **55** (2010) 2158–2162.
- 25) S.-J. Pan, W.-T. Tsai, J.-C. Kuo and I.-W. Sun: *J. Electrochem. Soc.* **160** (2013) D320–D325.
- 26) T. Hirato, J. Fransaer and J.-P. Celis: *J. Electrochem. Soc.* **148** (2001) C280–C283.
- 27) S. Shiomi, M. Miyake, T. Hirato and A. Sato: *Mater. Trans.* **52** (2011) 1216–1221.
- 28) M. Miyake, H. Motonami, S. Shiomi and T. Hirato: *Surf. Coat. Tech.* **206** (2012) 4225–4229.
- 29) S. Shiomi, M. Miyake and T. Hirato: *J. Electrochem. Soc.* **159** (2012) D225–D229.
- 30) A. Endo, M. Miyake and T. Hirato: *Electrochim. Acta* **137** (2014) 470–475.
- 31) M. Miyake, H. Fujii and T. Hirato: *Surf. Coat. Tech.* **277** (2015) 160–164.
- 32) M. Miyake, Y. Kubo and T. Hirato: *Electrochim. Acta* **120** (2014) 423–428.
- 33) A. Kitada, K. Nakamura, K. Fukami and K. Murase: *Electrochemistry* **82** (2014) 946–948.
- 34) A. Kitada, K. Nakamura, K. Fukami and K. Murase: *Electrochim. Acta* **211** (2016) 561–567.
- 35) I. Matsui, S. Ono, Y. Takigawa, T. Uesugi and K. Higashi: *Mater. Sci. Eng. A* **550** (2012) 363–366.
- 36) F. Endres, D. MacFarlane and A. Abbott (ed.): *Electrodeposition from Ionic Liquids*, (Wiley, Weinheim, 2008).
- 37) G.R. Stafford and C.L. Hussey: in *Advances in Electrochemical Science and Engineering, Volume 7*, ed. by R.C. Alkire and D.M. Kolb, (Wiley, Weinheim, 2002) pp. 275–347.
- 38) T. Tsuda: *J. Surf. Finish. Soc. Japan* **60** (2009) 497–501.
- 39) S. Shiomi, M. Miyake and T. Hirato: *J. Japan Inst. Light Met.* **63** (2013) 234–242.
- 40) M. Ueda: *J. Solid State Electrochem.* **21** (2017) 641–647.
- 41) Y. Gu, J. Liu, S. Qu, Y. Deng, X. Han and W. Hu: *J. Alloys Compd.*

- 690 (2017) 228–238.
- 42) T. Tsuda, G.R. Stafford and C.L. Hussey: *J. Electrochem. Soc.* **164** (2017) H5007–H5017.
- 43) A.A. Fannin, D.A. Floreani, L.A. King, J.S. Landers, B.J. Piersma, D.J. Stech, R.L. Vaughn and J.S. Wilkes: *J. Phys. Chem.* **88** (1984) 2614–2621.
- 44) A. Leyland and A. Matthews: *Wear* **246** (2000) 1–11.
- 45) A. Leyland and A. Matthews: *Surf. Coat. Tech.* **177–178** (2004) 317–324.
- 46) X. Li and B. Bhushan: *Mater. Charact.* **48** (2002) 11–36.
- 47) J. Hay, P. Agee and E. Herbert: *Exp. Tech.* **34** (2010) 86–94.
- 48) T. Rouxel: *J. Am. Ceram. Soc.* **90** (2007) 3019–3039.
- 49) P.K. Zysset, X. Edward Guo, C. Edward Hoffer, K.E. Moore and S.A. Goldstein: *J. Biomech.* **32** (1999) 1005–1012.
- 50) T. Tsuda, C.L. Hussey and G.R. Stafford: *J. Electrochem. Soc.* **152** (2005) C620–C625.
- 51) T. Tsuda, S. Arimoto and S. Kuwabata: *J. Electrochem. Soc.* **155** (2008) D256–D262.
- 52) J.G. Wang, B.W. Choi, T.G. Nieh and C.T. Liu: *J. Mater. Res.* **15** (2000) 798–807.
- 53) C.C. Yuan and X.K. Xi: *J. Appl. Phys.* **109** (2011) 033515.
- 54) C.A. Schuh, T.C. Hufnagel and U. Ramamurty: *Acta Mater.* **55** (2007) 4067–4109.
- 55) A.S. Argon: *Acta Metall.* **27** (1979) 47–58.
- 56) D. Pan, Y. Yokoyama, T. Fujita, Y.H. Liu, S. Kohara, A. Inoue and M.W. Chen: *Appl. Phys. Lett.* **95** (2009) 141909.